Understanding the Mechanism of the Antimitogenic Activity of Suramin†

Karuppanan Muthusamy Kathir,‡ Thallapuranam Krishnaswamy S. Kumar,‡ and Chin Yu*,‡,§

Department of Chemistry and Biochemistry, University of Arkansas, Fayetteville, Arkansas 72701, and Department of Chemistry, National Tsing Hua University, Hsinchu 30043, Taiwan

Received July 16, 2005; Revised Manuscript Received November 18, 2005

ABSTRACT: Fibroblast growth factors (FGFs) play crucial roles in the regulation of key cellular processes such as angiogenesis, differentiation, and tumor growth. Suramin, a polysulfonated naphthylurea, is known to be a potent inhibitor of FGF-induced angiogenesis. Using isothermal titration calorimetry, we demonstrate that human acidic fibroblast growth factor (hFGF-1) binds to suramin with high affinity in the nanomolar range. The suramin:hFGF-1 binding stoichiometry is estimated to be 2:1. Size-exclusion chromatography data reveal that suramin oligomerizes hFGF-1 to form a stable tetramer. Thermal unfolding experiments monitored by steady state fluorescence, and limited trypsin digestion analysis data suggest that suramin-induced oligomerization of hFGF-1 occurs in two steps. The first step involves the binding of suramin at specific sites on the protein. Two molecules of suramin appear to bind simultaneously to one molecule of hFGF-1. Binding of suramin possibly involves formation of solvent-exposed nonpolar surfaces in hFGF-1. In the second step, FGF appears to oligomerize through coalescence of the solvent-accessible nonpolar surfaces. Results of the NMR experiments reveal that suramin binds to residues in the heparin binding pocket as well as to residues involved in FGF receptor binding. On the basis of the results of this study, we propose a model to explain the molecular mechanism(s) underlying the antimitogenic activity of suramin. To our knowledge, this is the first study in which suramin interaction sites on FGF have been characterized.

The establishment and maintenance of vascular supply are vital for the growth of normal as well as neoplastic tissues (*1*). Angiogenesis is a cellular process that aids in the formation of new blood vessels via sprouting from preexisting vessels (*2*, *3*). This process is crucial for the development, progression, and metastasis of tumors (*2*, *4*). There are several positive modulators of angiogenesis, and fibroblast growth factors (FGFs)[1] are the most prominent among them. It is increasingly believed that angiogenesis is a potential therapeutic target for the control and treatment for a wide range of tumors (*5*−*7*). In this background, recently there have been intensive efforts to identify compounds that could effectively inhibit the angiogenic activity of FGFs (*4*, *6*, *8*).

FGFs are ∼16 kDa all-β-sheet proteins, devoid of disulfide bonds (*9*−*11*). The secondary structural elements in human acidic fibroblast growth factor (hFGF-1) consist of 12 β-strands organized into β-barrel architecture (*12*, *13*). hFGF-1 exhibits its cell proliferation activity by specifically binding to its transmembrane receptor (FGFR; *14*−*17*). Crystal structure data show that formation of the hFGF−FGFR binary complex requires participation of proteoglycans such as heparin (*18*, *19*). Heparin binds to both the ligand (hFGF-1) and the receptor with almost equal affinity ($K_d \sim 10^{-6}$ M) (*20*). Heparin is proposed to play an important role in the formation and stabilization of the ligand−receptor complex (*16*, *18*). Since the demonstration that FGF-mediated angiogenesis plays a crucial role in the progression and metastasis of tumors, there has been intensive research directed at the development of drugs that could effectively inhibit angiogenesis (*4*−*6*). Suramin ({carbonyl bis[imino-3,1-phenylenecarbonylimino(4-methyl-3,1-phenylene)carbonylimino]}-bis(1,3,5-naphthalenetrisulfonic acid) hexasodium salt) is the most well-known of the drugs that inhibit tumor growth (*9*). Suramin exhibits its antitumor activity in a number of cell lines (*21*, *22*). It is also under investigation for the treatment of several malignancies (*23*). However, very little is known about the molecular basis underlying the antitumor activity of suramin. Several studies using smaller structural units of suramin (such as sulfonated naphthalene derivatives) proposed that the drug (suramin) binds to the heparin binding pocket in hFGF-1 and consequently interferes with the interaction of the growth factor with its cell surface receptor (*4*−*6*, *9*). However, the antitumor activity of these minimalistic suramin derivatives is significantly lower than that exhibited by suramin. Therefore, understanding the molecular mechanism by which suramin inhibits the FGF-induced tumors is extremely important. In this context, in this study we investigate the structural interactions governing suramin−hFGF-1 interaction using a variety of biophysical techniques, including multidimensional NMR spectroscopy. Results obtained reveal that hFGF-1 binds strongly to suramin and forms a biologically inactive tetramer.

† This study was supported by grants from the National Institutes of Health (NIH NCRR COBRE Grant 1 P20 RR15569), the Department of Energy (Grant DE-FG02-01ER15161), the Arkansas Biosciences Institute, and the National Science Council, Taiwan.

* To whom correspondence should be addressed. E-mail: cyu@uark.edu. Tel: (479) 575-2724. Fax: (479) 575-4049.

‡ University of Arkansas.

§ National Tsing Hua University.

[1] Abbreviations: FGF, fibroblast growth factor; FGFR, fibroblast growth factor receptor; SOS, sucrose octasulfate; NMR, nuclear magnetic resonance; ITC, isothermal calorimetry, HSQC, heteronuclear single-quantum coherence.

10.1021/bi051389b CCC: $33.50
Published on Web 12/21/2005

MATERIALS AND METHODS

Plasmid DNA was prepared using a mini-prep kit obtained from Qiagen. EcoRI and XbaI were purchased from New England Biolabs. Ampicillin and chloramphenicol were procured from AMERSCO. Low-molecular weight heparin ($M_r \sim 3000$), phenylmethanesulfonyl fluoride, aprotinin, pepstatin, leupeptin, Triton X-100, β-mercaptoethanol, suramin, and trypsin were obtained from Sigma Chemical Co. Heparin−Sepharose was procured from Amersham Biosciences. All other chemicals used were of high-quality analytical grade. All solutions were prepared in Milli Q water. Unless otherwise mentioned, all experiments were performed in 10 mM Tris (pH 6.5) containing 100 mM NaCl.

Protein Purification. Recombinant hFGF-1 was prepared from transformed *Escherichia coli* BL21(DE3)pLysS cells. The expressed protein was purified on a heparin−Sepharose affinity column over a NaCl gradient (from 0 to 1.5 M). Desalting of the purified protein was achieved by ultrafiltration using an Amicon setup. The purity of the protein was assessed using SDS−PAGE. The authenticity of the sample was verified by ES-mass analysis. The concentration of the protein was estimated on the basis of its extinction coefficient value at 280 nm.

Preparation of Isotope-Enriched hFGF-1. Uniform ^{15}N isotope labeling (of human FGF-1) was achieved using M9 minimal medium containing $^{15}NH_4Cl$. To realize maximal expression yields, the composition of the M9 medium was modified by the addition of a mixture of vitamins. The expression host strain, *E. coli* BL21(DE3)pLysS, is a vitamin B_1-deficient host, and hence, the medium was supplemented with thiamine (vitamin B_1). Protein expression yields were in the range of 25−30 mg/L of the isotope-enriched medium. The extent of ^{15}N labeling was verified by ES-mass analysis.

Fluorescence Measurements. The thermodynamic stability of hFGF-1 was assessed from the thermal denaturation experiments. Fluorescence spectra were measured on a Hitachi F-2500 fluorimeter at 5 or 10 nm resolution, using an excitation wavelength of 280 nm. Unless otherwise mentioned, all fluorescence measurements were made using a protein concentration of 100 μg/mL in 10 mM Tris containing 100 mM NaCl (pH 6.5). The fraction of unfolded species was estimated from the ratio of the emission intensities at 308 and 350 nm.

NMR Experiments. NMR experiments were performed on a Bruker 700 MHz and 500 MHz spectrometers (cryoprobe). For the two-dimensional heteronuclear experiments, the concentration of the protein used was ~0.5 mM. The protein samples were prepared in 10 mM Tris buffer containing 100 mM sodium choloride (pH 6.5). All NMR data were acquired at 25 ± 0.5 °C.

Proteolytic Activity. Protection of hFGF-1 by suramin against the action of trypsin was evaluated by incubating hFGF-1 at a concentration of 0.5 mg/mL (in the presence and absence of various molar ratios of suramin) with 0.05 mg/mL trypsin in 10 mM Tris buffer containing 100 mM NaCl. The action of trypsin was stopped by heating the mixture at 90 °C for ~10 min. The products of the protease action(s) were analyzed by SDS−PAGE. The degree of protection offered by suramin was estimated by measuring the intensity of the band (on SDS−PAGE) corresponding to hFGF-1 (remaining after protease digestion) using a scanning densitometer. The intensity of the band corresponding to hFGF-1 not subjected to protease treatment was considered as a control for 100% protection.

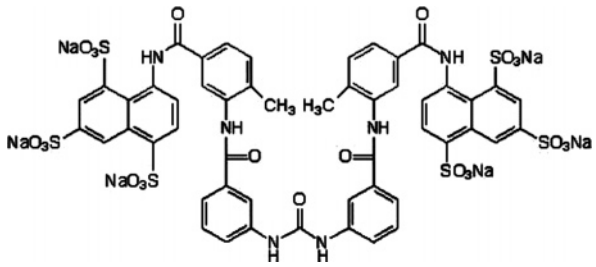

FIGURE 1: Chemical structure of suramin.

Isothermal Titration Calorimetry (ITC). ITC experiments were performed using a VP-ITC calorimeter (Microcal Inc., Northampton, MA). All experiments were performed at 298 K. The sample cell was filled with an ~50 μM solution of hFGF-1 (volume, 1.4 mL). Suramin (10 times more concentrated) was titrated into the cell from the 250 μL syringe, the contents of which were stirred at 310 rpm. A typical experiment consisted of 40 successive automatic injections of 6 μL each with a 240 s equilibration time between the injections. The first injection consisted of 6 μL and was ignored in the final data analysis. The heat change for the dilution of the ligand injections was measured by injecting suramin into the buffer under identical conditions and was subtracted from the measured heat change of binding of ligand to protein. Data analysis was performed using the least-squares method to determine the equilibrium binding constant (K_d), the enthalpy of complex formation (ΔH), and the entropy (ΔS) of the reaction.

RESULTS AND DISCUSSION

Suramin is asymmetrical polysulfonated naphthylurea that has been successfully used to cure a wide array of disorders such as trypanosomiasis and onchocerciaisis (Figure 1; *23*). Suramin and its derivatives have been shown to possess potent antitumor activity (*4*−*6*). The antimitogenic activity of suramin is believed to stem from its ability to bind to FGFs and disrupt interaction with their cell surface receptors.

Suramin Binds to hFGF-1. Isothermal titration calorimetry (ITC) is a versatile technique for characterizing protein−protein or protein−ligand interactions (*24*). ITC experiments provide direct information about the stoichiometry, affinity, and enthalpy of protein−ligand binding reactions in solution (*25*). The binding isotherm characterizing suramin−hFGF-1 interaction is nearly sigmoidal (Figure 2A). The binding isotherm fits best to a two-site binding model yielding binding constant values of ~54 and ~555 nM, respectively. The binding stoichiometry for the suramin−hFGF-1 interaction is ~2:1 (Figure 2A). The binding of hFGF-1 and the drug proceeds with a negative enthalpy ($\Delta H \sim -13.3$ kcal/mol). Increasing the protein concentration has little or no effect on the thermodynamic parameters characterizing hFGF-1−suramin interaction(s). The results of ITC experiments clearly show that hFGF-1 interacts strongly with suramin, and one molecule of the protein appears to bind two molecules of the suramin. The binding affinity shared by suramin and FGF was examined at various concentrations of NaCl in an effort to understand the nature of forces (electrostatic or nonpolar) stabilizing the suramin−FGF

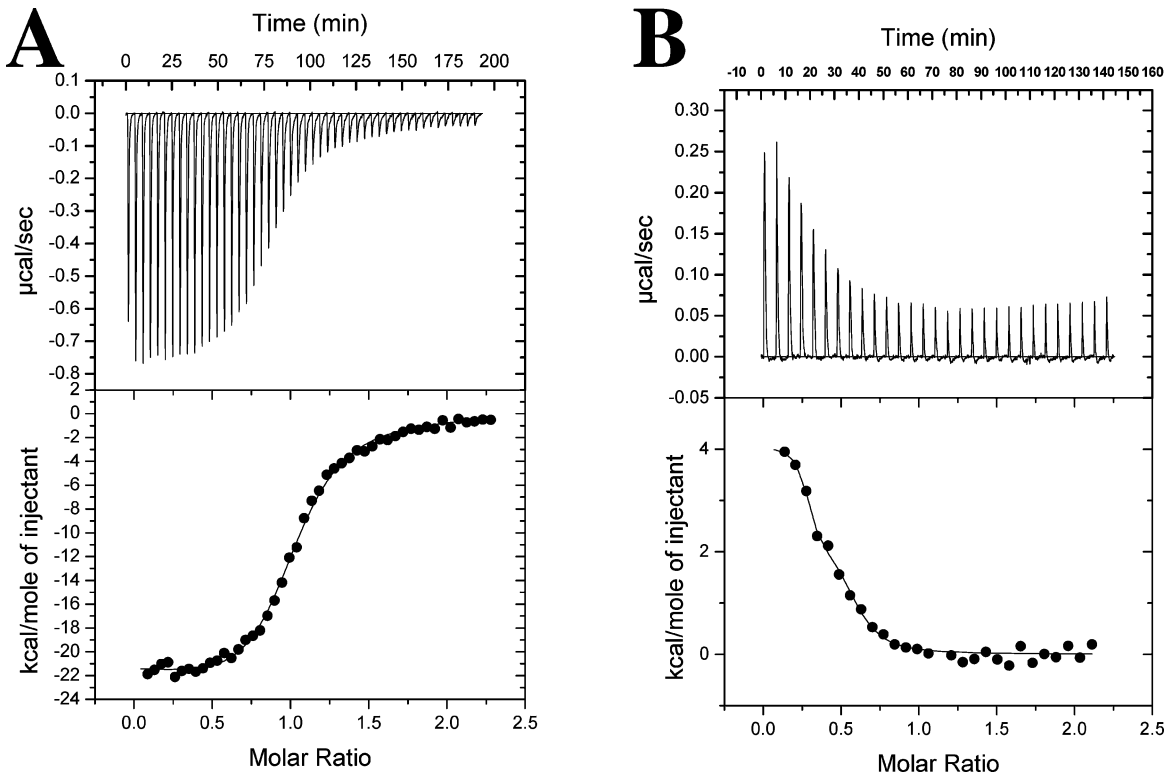

FIGURE 2: Binding isotherm of the titration of hFGF-1 with suramin at 100 mM NaCl (A) and 1 M NaCl (B). The top panel represents the raw data for the titration. The bottom panel shows the integrated data obtained from the raw data after subtraction of the heats of dilution. The solid line in the bottom panel represents the best curve fit to the data using a two-independent site model. The binding constant characterizing the suramin−hFGF-1 interaction equals ∼54 nm in 100 mM NaCl.

interaction. The binding isotherm representing the suramin−FGF interaction shows that the drug interacts with FGF even at high salt concentrations (1 M NaCl, Figure 2B). Interestingly, the sign of the enthalpy change (ΔH) accompanying the suramin−FGF interaction is reversed (from −13.3 to 2.25 kcal/mol) when the NaCl concentration is increased from 100 mM to 1 M (Figure 2B). These results suggest that at a low salt concentration, suramin−FGF interaction is stabilized by both electrostatic and nonpolar interactions. However, at a higher NaCl concentration (1 M NaCl), the electrostatic interactions are nullified and the suramin−FGF interaction is largely stabilized by nonpolar interactions. This explains the switch of the drug−FGF interaction from being exothermic (at low salt concentrations) to endothermic (at high salt concentrations).

Suramin Binds and Oligomerizes FGF-1. Size-exclusion chromatography is a useful technique for monitoring the change(s) in molecularity of proteins upon ligand−protein interactions. Fibroblast growth factors have been shown to have a tendency to oligomerize upon binding to suramin (*8*). In this context, we studied the effect(s) of suramin on the molecularity of hFGF-1 using size-exclusion chromatography. hFGF-1 in the absence of suramin elutes as a single peak with an elution time of ∼75.6 min (Figure 3A). Extrapolation of this elution time on the standard plot (of log molecular mass vs elution time) yields a molecular mass of ∼15.9 kDa that corresponds to the monomeric state of hFGF-1 (Figure 3E). The elution profile of hFGF-1 in the presence of suramin (at a suramin:hFGF-1 molar ratio of 0.5:1.0) shows two peaks, one representing free hFGF-1 (with an elution time of 75.6 min) and the other smaller peak corresponding to the tetrameric form (with an elution time of ∼47.05 min) of the protein with an estimated molecular mass of ∼65 kDa (Figure 3B). The peak representing the tetramer further increases in intensity at a drug:protein ratio of 0.75:1.0 (Figure 3C). At a suramin:hFGF-1 ratio of 2.0:1.0, the protein predominantly exists as a tetramer as evidenced by a single peak (with an elution time of ∼47.0 min) in the elution profile (Figure 3D). Interestingly, oligomerization of hFGF-1 induced by suramin appears to be highly cooperative as no stable intermediate state(s) in the oligomerization reaction could be detected. Therefore, the size-exclusion chromatography data clearly demonstrate that hFGF-1 binds to suramin and oligomerizes the protein to a tetrameric form. Suramin-induced oligomerization of hFGF-1 has also been observed in other studies, but the molecular size of the oilgomer has not been unambiguously characterized (*8*).

Oligomerization Induced by Suramin Occurs in Two Steps. hFGF-1 contains a single tryptophan residue at position 121 (*11*, *13*). The fluorescence spectrum of hFGF-1 in its native state shows an emission maximum around 308 nm (Figure 4, inset). The fluorescence of the lone tryptophan residue is almost completely quenched in the native state (Figure 4, inset). The quenching effect is attributed to the presence of proline and histidine residues in spatial proximity to the indole ring of tryptophan in the three-dimensional structure of hFGF-1 (*8*). However, this quenching effect is relieved in the denatured state(s) of the protein in 8 M urea (Figure 4, inset). The protein in its denatured state(s) shows an emission maximum around 350 nm. These spectral features are ideal for monitoring the global conformational changes that occur during the unfolding of the protein. We studied the effect(s) of suramin on the thermodynamic stability of

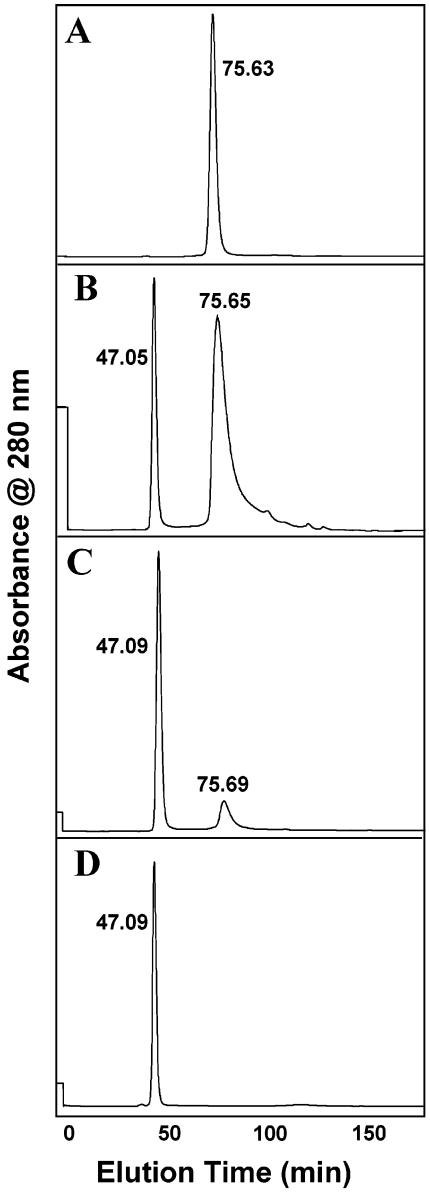

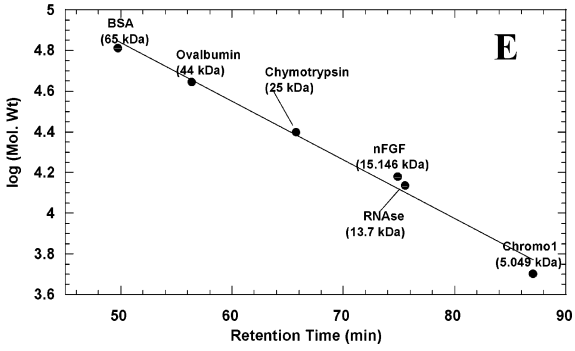

FIGURE 3: Size-exclusion chromatography of hFGF-1 obtained at various hFGF-1:suramin molar ratios: (A) 1:0, (B) 1.0:0.5, (C) 1.0:0.75, and (D) 2.0:1.0. (E) Plot of the logarithm of the molecular weights of proteins vs the elution times of the proteins. The numbers at the top of each fraction represent their elution times. The values in parentheses in panel E represent the molecular masses of the proteins in kilodaltons. The elution flow rate is 1 mL/min. The elution of proteins was monitored by their absorbance at 280 nm. The concentration of protein is ~1 mg/mL. Elution buffer used consists of 10 mM Tris containing 100 mM NaCl. BSA and nFGF-1 are abbreviations for bovine serum albumin and acidic fibroblast growth factor from newt (*Notopthalmus viridescens*), respectively.

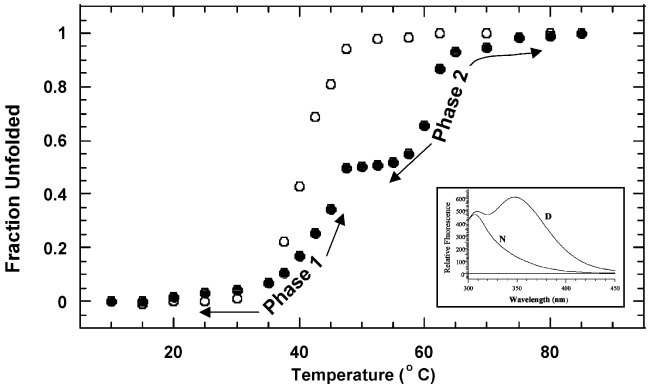

FIGURE 4: Thermal unfolding of hFGF-1 in the absence of suramin (○) and in the presence of suramin (at a suramin:hFGF-1 molar ratio of 2:1). The inset shows the fluorescence spectra of hFGF-1 in its native (N) and denatured (D) states. Unfolding in the presence of suramin proceeds in two phases. The first phase possibly represents the dissociation of the suramin-induced oligomer of hFGF-1. The second phase possibly indicates the unfolding of the dissociated monomers of hFGF-1. Thermal unfolding experiments were performed at a protein concentration of 100 μM. The excitation and emission slit widths were set at 5 and 10 mm, respectively. Fluorescence spectra were acquired upon excitation at 280 nm.

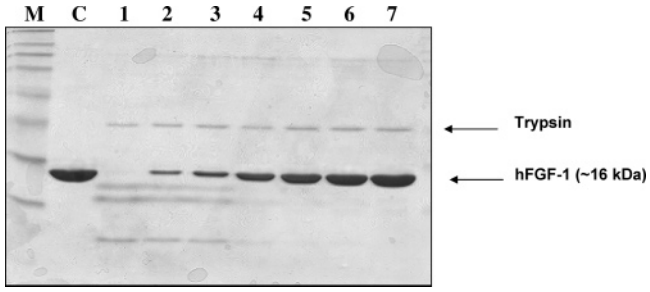

FIGURE 5: SDS−PAGE of hFGF-1 in the presence of suramin. Lane M contained the molecular mass markers. Lane C contained hFGF-1 in the absence of trypsin. Lanes 1−7 contained the trypsin cleavage products obtained at suramin:hFGF-1 molar ratios of 0.0:1.0, 0.1:1.0, 0.2:1.0, 0.5:1.0, 0.75:1.0, 1:1.0, and 2:1.0, respectively. Enhanced protection of the protein (hFGF-1) from trypsin cleavage with the increase in suramin concentration suggests that the protein oligomerizes in the presence of the suramin.

the protein by equilibrium thermal denaturation monitored by changes in the ratio of 350 nm:308 nm fluorescence.

The unfolding of the protein under these conditions appears to be cooperative with no detectable accumulation of equilibrium intermediates. Complete unfolding of the protein occurs beyond 50 °C (Figure 4). The T_m [temperature at which 50% of the molecules exist in the unfolded state(s)] for the unfolding reaction is estimated to be ~40 °C. Interestingly, temperature-induced unfolding of hFGF-1 in the presence of saturating concentrations of suramin (at a FGF-1:suramin ratio of 1:2) occurs in two discrete phases (Figure 4). In the presence of the suramin, the protein appears to undergo little or no structural change below 30 °C. Beyond this temperature, the 350 nm:308 nm fluorescence ratio increases significantly, suggesting progressive unfolding of the protein (Figure 4). The unfolding profile reaches a plateau at 47 °C, and the 350 nm:308 nm fluorescence ratio does not significantly change up to 60 °C. The second phase of unfolding begins beyond 60 °C, and the changes in the 350 nm:308 nm fluorescence ratio are completed as the temperature reaches 70 °C (Figure 4). The first phase of unfolding possibly represents the dissociation of the suramin-induced

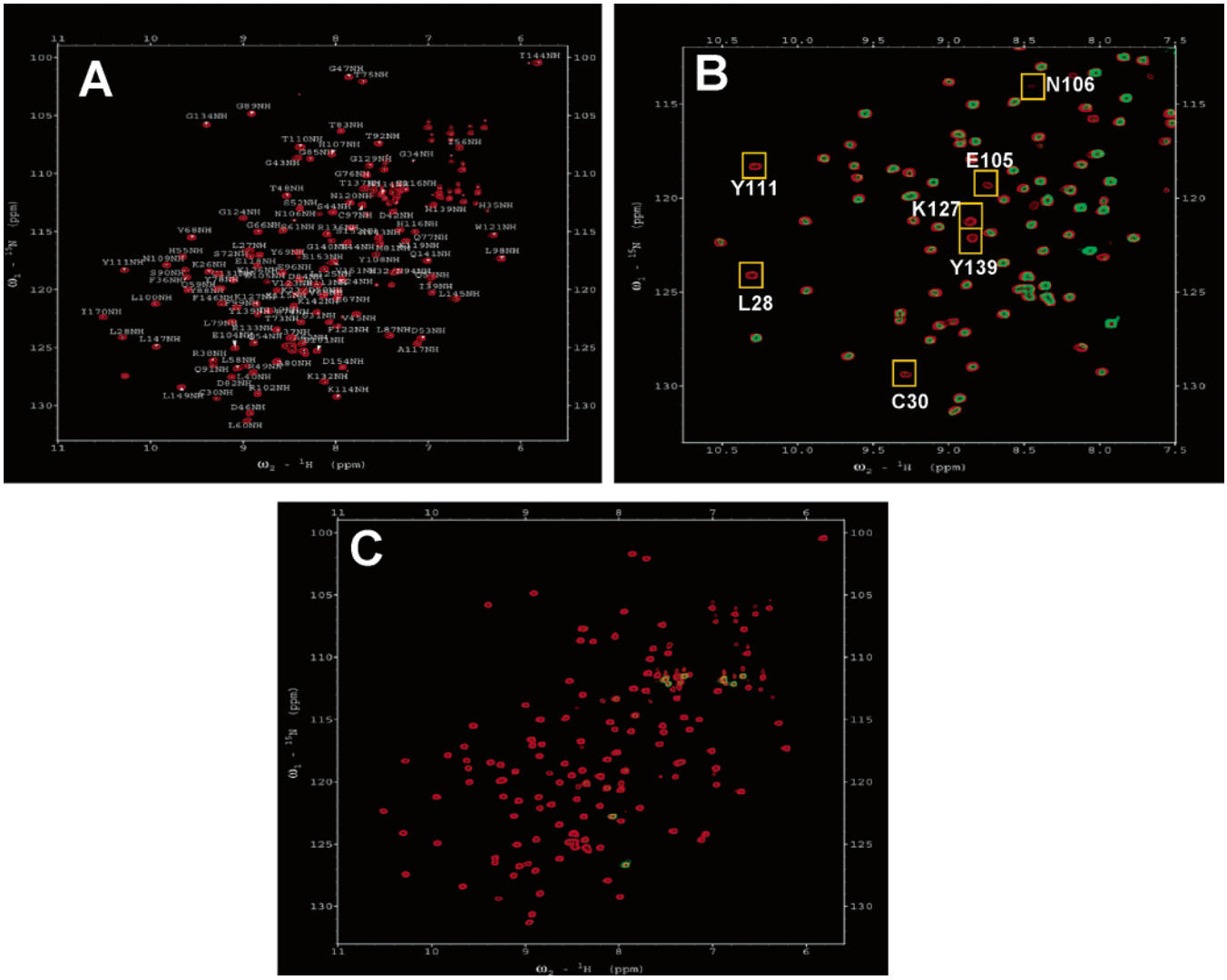

FIGURE 6: $^{1}H-^{15}N$ HSQC spectra of hFGF-1 in the absence and presence of suramin. (A) HSQC spectrum of hFGF-1 in the absence of suramin. (B) Overlap of the HSQC spectra of hFGF-1 in the absence (red) and presence of suramin (green) (at a suramin:hFGF-1 molar ratio of 0.6:1.0). The yellow boxed areas represent selected cross-peaks of residues that disappear in the presence of suramin. (C) Overlap of the HSQC spectra of hFGF-1 in the absence (red) and presence of suramin (green) at a suramin:hFGF-1 molar ratio of 2:1. It could be observed in the presence of suramin that most of the $^{1}H-^{15}N$ cross-peaks in the spectrum disappear, suggesting that the drug induces oligomerization of the protein. All HSQC spectra were acquired at 298 K in 10 mM Tris containing 100 mM NaCl.

oligomer to the partially structured monomeric hFGF units. In the second phase, the partially structured monomeric state unfolds to the completely denatured state(s) of the protein. The two-phase thermal unfolding profile of hFGF-1 in the presence of suramin is consistent with the size-exclusion chromatography data that suggest that suramin binds and induces oligomerization of the hFGF-1.

Limited proteolytic digestion is a useful technique for monitoring conformational flexibility of proteins and map protein−ligand and protein−protein binding interfaces (*26*, *27*). We used limited trypsin digestion to study the presumptive structural transitions induced in hFGF-1 upon binding to suramin. hFGF-1 is rich in lysine and arginine residues (*11*−*13*). As the putative cleavage sites for trypsin corresponds to the carbonyl ends of lysine and arginine residues, trypsin is an apt choice for following the conformational changes induced in hFGF-1 at various concentrations of suramin. Undigested hFGF-1 yields a band on SDS−PAGE that corresponds to a molecular mass of 16 kDa (Figure 5, lane C). The intensity of the band (after Coomassie staining) is used as a control to monitor the susceptibility of the protein to trypsin cleavage. In the absence of suramin, more than 90% of the ~16 kDa band is cleaved within 30 min of initiation of trypsin cleavage (Figure 5, lane 1). At low suramin:hFGF-1 molar ratios, the cleavage pattern of the protein is different from that observed in the absence of the suramin (Figure 5). Some of the low-molecular mass cleavage products observed in the absence of suramin are missing in the presence of suramin. The observed differences possibly arise due to steric masking of some of the potential enzyme cleavage sites by suramin and/or due to conformational changes induced in the protein upon suramin binding. Interestingly, the intensity of the 16 kDa band, corresponding to the undigested hFGF-1, increases with the increase in the drug:protein ratio (Figure 5). This observation is consistent with the increase in the population of the hFGF-1 oligomer(s) formed at higher molar ratios of suramin to the protein. We could not observe any band corresponding to the tetramer or oligomer on SDS−PAGE, which probably indicates that the suramin-induced oligomer(s) of hFGF-1 is stabilized by noncovalent interactions between the monomeric hFGF-1 units. These noncovalent stabilizing forces appear to be

disrupted under conditions used during SDS−PAGE. In addition, it is important to mention that control experiments with bovine serum albumin revealed that the suramin does not affect the activity of trypsin (data not shown). In summary, both the size-exclusion chromatography data and the results of the limited proteolytic digestion experiments clearly show that suramin binds specifically to hFGF-1 and induces oligomerization of the protein.

Characterization of the Suramin Binding Sites in hFGF-1. The $^{1}H-^{15}N$ HSQC spectrum serves as a fingerprint of the backbone conformation of a protein (*28*). Chemical shift perturbation or disappearance of $^{1}H-^{15}N$ cross-peaks in the $^{1}H-^{15}N$ HSQC spectrum, upon addition of a ligand or a protein partner, not only provides useful information about protein−ligand/protein interaction(s) but also sheds light on the conformational changes that possibly accompany ligand (drug) binding (*29*). In this context, we mapped the putative suramin binding sites on hFGF-1 on the basis of changes observed in the $^{1}H-^{15}N$ HSQC spectra obtained at various drug:protein molar ratios. In total, 10 $^{1}H-^{15}N$ HSQC spectra were acquired at suramin:hFGF-1 ratios ranging from 0:1 to 4:1. $^{1}H-^{15}N$ HSQC spectra of hFGF-1 in the absence of suramin are well-dispersed, and the cross-peaks representing the backbone amide protons of the 126 residues in the protein have been unambiguously assigned (*11*, *12*). No significant changes could be discerned in the $^{1}H-^{15}N$ HSQC spectra acquired at suramin:hFGF-1 molar ratios lower than 0.3−1 (Figure 6A). At a suramin:hFGF-1 ratio of 0.6:1.0, cross-peaks corresponding to 10 residues, including Leu28, Cys30, Gly34, His35, Glu105, Asn106, Tyr111, Lys127, Tyr139, and Lys142, completely disappear (Figure 6B). These residues possibly constitute the suramin binding site(s) in hFGF-1. Loss in intensities of selected cross-peaks in the $^{1}H-^{15}N$ HSQC spectrum with suramin appears to be due to an intermediate rate of chemical exchange between hFGF-1 and suramin on the NMR time scale (*30*). In general, in case of an intermediate chemical exchange rate, the frequencies of the changing resonances become poorly defined and extensive kinetic broadening sets in. When the lines become sufficiently broad, the resonances completely disappear in the $^{1}H-^{15}N$ HSQC spectra (*30*). The putative suramin binding sites are distributed in two locations in the three-dimensional structure of hFGF-1. Lys127, Tyr139, and Lys142 are located in the heparin binding pocket (Figure 7). Leu28, Cys30, Gly34, and His35 constitute the second cluster of residues that bind to suramin and are involved in the FGF−FGFR interface (Figure 7). In marked contrast, binding studies using several smaller structural analogues of suramin, including sulfonated naphthalene derivatives, showed that the suramin derivatives are directed only to the hFGF-1−heparin binding interface (*4*−*6*, *9*, *33*). Therefore, it appears that the smaller derivatives of suramin do not completely mimic the binding interactions of suramin with hFGF-1. This aspect probably accounts for the potency of the minimalistic derivatives of suramin being lower than that of suramin itself (*4*). The presence of two discrete suramin binding sites is also supported by ITC data, which show that hFGF-1 binds to suramin even in the presence of saturating amounts of sucrose octasulfate (SOS) which mimics the action of heparin in supporting the FGF-induced mitogenic activity (Figure S1 of the Supporting Information). The binding affinity shared by the suramin and the protein

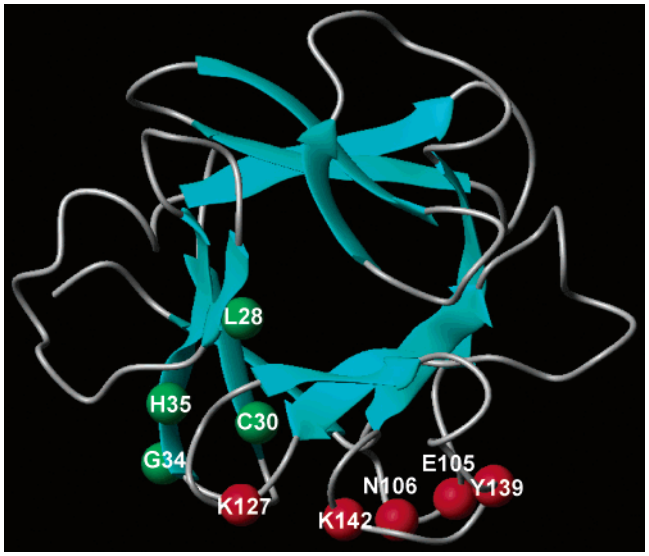

FIGURE 7: Model of the structure of hFGF-1 showing the residues whose resonances disappear in the $^{1}H-^{15}N$ HSQC spectrum of the protein obtained at a suramin:hFGF-1 molar ratio of 0.6:1.0. Suramin appears to bind residues in the heparin binding pocket (red balls) as well as residues (L28, C30, G34, and H35) that make up the FGF−FGFR interface (green balls).

decreases only marginally in the presence of SOS. At suramin:hFGF-1 molar ratios greater than 2:1, more than 90% of the cross-peaks in the $^{1}H-^{15}N$ HSQC spectra disappear possibly due to the oligomerization induced by the suramin (Figure 6C). Oligomerization dramatically alters the transverse relaxation rates (T_2) of resonances, resulting in broadening of peaks leading to random and widespread disappearance of peaks in the $^{1}H-^{15}N$ HSQC spectra. The results of the NMR experiments demonstrate that at low suramin:hFGF-1 molar ratios (∼0.6:1.0), the drug (suramin) binds at two distinct sites, one constituting the heparin binding site and the other comprising residues that are involved in FGF receptor binding. The bound suramin ultimately induces oligomerization of the protein.

Mechanism of Action of Suramin. It is important to understand the mechanism underlying the antimitogenic activity of suramin. There are at least two possible mechanisms by which suramin inhibits the mitogenic activity of hFGF-1. FGFs exhibit their cell proliferation activity by binding to their transmembrane tyrosine kinase receptors.

Results of the isothermal titration calorimetry experiments reveal that suramin binds strongly to FGF ($K_d \sim 54$ nm) in a 2:1 ratio. $^{1}H-^{15}N$ HSQC data show that suramin binds to two distinct sites on the FGF molecule, one located in the heparin binding pocket and the other site located in the region between β-strands I and II. Our preliminary docking studies reveal that the two suramin binding sites are separated by a distance of ∼32 Å, and therefore, a single suramin molecule (with a length of ∼24 Å) cannot bind simultaneously to both binding sites. As the suramin molecule is symmetric, it is logical to assume that two suramin molecules can simultaneously bind to one FGF molecule (Figure 8). Results of the thermal unfolding experiments suggest that the formation of the FGF-1 tetramer occurs in two cooperative steps. The first step appears to be the binding of the drug molecule (suramin) to FGF (Figure 8). Far-UV and near-UV CD data suggest that the binding of suramin induces subtle conformational change(s) in FGF, possibly exposing nonpolar

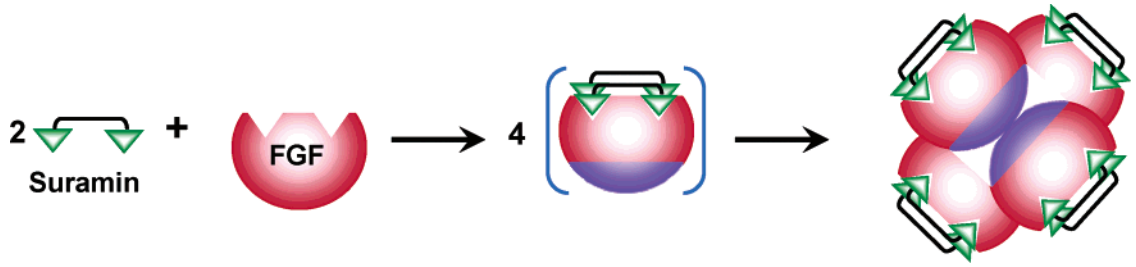

FIGURE 8: Cartoon depicting the primary mechanism by which suramin exerts its antimitogenic activity. Suramin binding residues in FGF-1 exist (red) in two clusters. One cluster consisting of residues Lys127, Tyr139, and Lys142 constitutes the heparin binding site. The second cluster of residues Leu28, Cys30, and Gly34 that bind to suramin are also involved in receptor binding. Formation of the suramin-induced FGF tetramer appears to occur in two steps. The first step involves the binding of two molecules of suramin to a molecule of FGF. Binding of suramin appears to induce a subtle conformation in FGF-1 possibly involving the formation of solvent-accessible nonpolar surfaces (violet). The FGF tetramer occurs spontaneously due to coalescence of the solvent-exposed nonpolar surfaces in FGF monomers. In the second step, FGF (red) binds to the cell surface receptor, resulting in the activation of the signaling process. Suramin has affinity for both FGF and its receptor (blue). The drug binds at the FGF−receptor interface and inhibits the cell proliferation activity.

surfaces in the protein to the solvent (data not shown). The second step plausibly is the spontaneous formation of the biologically inactive FGF tetramer due to coalescence of the transiently formed solvent-exposed nonpolar surfaces in each of the FGF monomers (Figure 8). The FGF tetramer that is formed is biologically inactive as it is incapable of binding to the cell surface receptor.

Although suramin appears to exhibit its action by primarily inducing oligomerization of FGF, there could be other alternative mechanisms by which the drug exerts its antimitogenic activity. FGF exhibits its cell proliferation activity by binding to its receptor (FGFR). Crystal structure data show that most of the FGF−FGFR interactions are contributed by the D2 domain of the receptor (Figure S2 of the Supporting Information). In this context, suramin could physically bind to residues (in both FGF and FGFR) at the FGF−FGFR binding interface and sterically block the interaction of the growth factor with its cell surface receptor (*34*). This mode of action of suramin is supported by several lines of evidence. (1) $^{15}N-^{1}H$ chemical shift perturbation data show that suramin binds to residues (Leu28, Cys30, Gly34, and His35) in hFGF-1 that are involved in the FGF−receptor interface (*31*, *32*). (2) The binding isotherm representing the interaction of suramin and the D2 domain (of FGFR) reveals that the drug binds to the receptor domain with high affinity ($K_d = 1.06 \times 10^{-6}$ M) (Figure S3A of the Supporting Information). (3) ITC data reveal that suramin cannot bind to a preformed FGF−D2 domain binary complex (Figure S3B of the Supporting Information). These results suggest that suramin binds to residues involved in the FGF−D2 domain binding interface. The mechanisms proposed for the antiangiogenic activity need to be further validated with more detailed studies characterizing the structure of the FGF−suramin−D2 domain ternary complex. Nevertheless, the results of the study provide useful clues for the design of more potent and less toxic therapeutic principles against several FGF-induced pathogeneses.

SUPPORTING INFORMATION AVAILABLE

Isothermograms representing the titration of hFGF-1 with sucrose octasulfate and hFGF-1 with suramin in the presence of saturating concentrations of SOS (Figure S1), isothermogram representing the binding of the D2 domain and hFGF-1 (Figure S2), binding of suramin and the D2 domain of the FGF receptor monitored by isothermal titration calorimetry (Figure S3A), and titration of the FGF−D2 domain binary complex with suramin (Figure S3B). This material is available free of charge via the Internet at http://pubs.acs.org.

REFERENCES

1. Cao, Y. (2004) Antiangiogenic cancer therapy, *Semin. Cancer Biol. 14*, 139−145.
2. Burgess, W. H., and Maciag, T. (1989) The heparin-binding (fibroblast) growth factor family of proteins, *Annu. Rev. Biochem. 58*, 575−606.
3. Folkman, J., and Klagsburn, M (1987) Angiogenic factors, *Science 235*, 442−447.
4. Manetti, F., Corelli, F., and Botta, M. (2000) Fibroblast growth factors and their inhibitors, *Curr. Pharm. Des. 6*, 1897−1924.
5. Sola, F. L., Capolonga, D., Moneta, P., Ubezio, P., and Grandi, M. (1999) *Cancer Chemother. Pharmacol. 36*, 217−222.
6. Zamai, M., Hariharan, C., Pines, D., Safran, M., Yayon, A., Caiolfa, V. R., Cohen-Luria, R., Pines, E., and Parola, A. H. (2002) Nature of interaction between basic fibroblast growth factor and the antiangiogenic drug 7,7-(carbonyl-bis[imino-*N*-methyl-4,2-pyrrolecarbonylimino[*N*-methyl-4,2-pyrrole]-carbonylimino])-bis-(1,3-naphthalene disulfonate). II. Removal of polar interactions affects protein folding, *Biophys. J. 82*, 2652−2664.
7. Song, S., Wientjes, M. G., Gan, Y., and Au, J. L. S. (2000) Fibroblast growth factors: An epigenetic mechanism of broad spectrum resistance to anticancer drugs, *Proc. Natl. Acad. Sci. U.S.A. 97*, 8658−8663.
8. Middaugh, C. R., Mach, H., Burke, C. J., Volkin, D. B., Dabora, J. M., Tsu, P. K., Brunner, M. W., Ryan, J. A., and Marfia, K. E. (1992) Nature of the interaction of growth factors with suramin, *Biochemistry 31*, 9016−9024.
9. Lozano, R. M., Jimenez, M. A., Santora, J., Rico, M., and Gallego, G. G. (1998) Solution structure of acidic fibroblast growth factor bound to 1,3,6-naphthalenetrisulfonate: A minimal model for the anti-tumoral action of suramins and suradistas, *J. Mol. Biol. 281*, 899−915.
10. Arunkumar, A. I., Kumar, T. K., Kathir, K. M., Srisailam, S., Wang, H. M., Leena, P. S., Chi, Y. H., Chen, H. C., Wu, C. H., Wu, R. T., Chang, G. G., Chiu, I. M., and Yu, C. (2002) Oligomerization of acidic fibroblast growth factor is not a prerequisite for its cell proliferation activity, *Protein Sci. 11*, 1050−1061.
11. Chi, Y. H., Kumar, T. K. S., Kathir, K. M., Lin, D. H., Zhu, G., Chiu, I. M., and Yu, C. (2002) Investigation of the structural stability of the human acidic fibroblast growth factor by hydrogen−deuterium exchange, *Biochemistry 41*, 15350−15339.
12. Ogura, K. K., Nagata, H., Hatanaka, H., Habuchi, K., Kimata, S., Tata, S., Raveral, M. W., Jaye, J., Schlessinger, J., and Inagaki, F. (1999) Solution structure of human acidic fibroblast growth factor and interaction with heparin-derived hexasaccharide, *J. Biomol. NMR 13*, 11−24.
13. Arunkumar, A. I., Srisailam, S., Kumar, T. K., Kathir, K. M., Chi, Y. H, Wang, H. M., Chang, G. G., Chiu, I., and Yu, C. (2002) Structure and stability of an acidic fibroblast growth factor from *Notophthalmus viridescens*, *J. Biol. Chem. 277*, 46424−46432.

14. Schlessinger, J. (2004) Common and distinct elements in cellular signaling via EGF and FGF receptors, *Science 306*, 1506−1507.
15. Plotnikov, A. N., Hubbard, S. R., Schlessinger, J., and Mohammadi, M. (2000) Crystal structures of two FGF−FGFR complexes reveal the determinants of ligand−receptor specificity, *Cell 101*, 413−424.
16. Pellegrini, L. (2001) Role of heparan sulfate in fibroblast growth factor signalling: A structural view, *Curr. Opin. Struct. Biol. 11*, 629−634.
17. Hung, K. W., Kumar, T. K., Chi, Y. H., Chiu, I. M., and Yu, C. (2004) Molecular cloning, overexpression, and characterization of the ligand-binding D2 domain of fibroblast growth factor receptor, *Biochem. Biophys. Res. Commun. 317*, 253−258.
18. Schlessinger, J., Plotnikov, A. N., Ibrahimi, O. A., Eliseenkova, A. V., Yeh, B. K., Yayon, A., Linhardt, R. J., and Mohammadi, M. (2000) Crystal structure of a ternary FGF−FGFR−heparin complex reveals a dual role for heparin in FGFR binding and dimerization, *Mol. Cell 6*, 743−750.
19. Yeh, B. K., Eliseenkova, A. V., Plotnikov, A. N., Green, D., Pinnell, J., Polat, T., Gritli-Linde, A., Linhardt, R. J., and Mohammadi, M. (2002) Structural basis for activation of fibroblast growth factor signaling by sucrose octasulfate, *Mol. Cell. Biol. 22*, 7184−7192.
20. Pantoliano, M. W., Horlick, R. A., Springer, B. A., Van Dyk, D. E., Tobery, T., Wetmore, D. R., Lear, J. D., Nahapetian, A. T., Bradley, J. D., and Sisk, W. P. (1994) Multivalent ligand−receptor binding interactions in the fibroblast growth factor system produce a cooperative growth factor and heparin mechanism for receptor dimerization, *Biochemistry 33*, 10229−10248.
21. Wang, L., Li, J. J., Zheng, Z. B., Liu, H. X., Du, G. J., and Li, S. (2004) Antitumor activities of a novel indolin-2-ketone compound, Z24: More potent inhibition on bFGF-induced angiogenesis and bcl-2 over-expressing cancer cells, *Eur. J. Pharmacol. 502*, 1−10.
22. Zhao, L., Wientjes, M. G., and Au, A. L. (2004) Evaluation of combination chemotherapy: Integration of nonlinear regression, curve shift, isobologram, and combination index analyses, *Clin. Cancer Res. 10*, 7994−8004.
23. Song, S., Yu, B., Wei, Y., Wientjes, M. G., and Au, J. L. (2004) Low-Dose Suramin Enhanced Paclitaxel Activity in Chemotherapy-Naïve and Paclitaxel-retreated Human Breast Xenograft Tumors, *Clin. Cancer Res. 10*, 6058−6065.
24. Brown, P. H., and Beckett, D. (2005) Use of inding enthalpy to drive an allosteric transition, *Biochemistry 44*, 3112−3121.
25. Banerjee, M., Poddar, A., Mitra, G., Surolea, A., Owa, T., and Battacharyya, B. (2005) Sulfonamide drugs binding to the colchicine site of tubulin: Thermodynamic analysis of the drug-tubulin interactions by isothermal titration calorimetry, *J. Med. Chem. 48*, 547−555.
26. Selwood, T., Smolensky, H., McCaslin, D. R., and Schechter, N. M. (2005) The interaction of human tryptase-β with small molecule inhibitors provides new insights into the unusual functional instability and quaternary structure of the protease, *Biochemistry 44*, 3580−3590.
27. Weisshart, K., Friedl, S., Taneja, P., Nasheuer, H. P., Schlott, B., Grosse, F., and Fanning, E. (2004) Partial Proteolysis of Simian Virus 40 T Antigen Reveals Intramolecular Contacts between Domains and Conformation Changes upon Hexamer Assembly, *J. Biol. Chem. 279*, 38943−38951.
28. Hajduk, P. J., Meadows, R. P., and Fesik, S. W. (1999) NMR-based screening in drug discovery, *Q. Rev. Biophys. 32*, 211−240.
29. Yu, L., Oost, T. K., Schkerjantz, J. M., Yang, J., Janowick, D., and Fesik, S. W. (2003) Discovery of aminoglycoside mimetics by NMR-based screening of *Escherichia coli* A-site RNA, *J. Am. Chem. Soc. 125*, 4444−4450.
30. Zuiderweg, E. R. (2002) Mapping protein−protein interactions in solution by NMR spectroscopy, *Biochemistry 41*, 1−7.
31. Pellegrini, L., Burke, D. F., von Delft, F., Mulloy, B., and Blundell, T. L. (2000) Crystal structure of fibroblast growth factor receptor ectodomain bound to ligand and heparin, *Nature 407*, 1029−1034.
32. Schlessinger, J., Plotnikov, A. N., Ibrahimi, O. A., Eliseenkova, A. V., Yeh, B. K., Yayon, A., Linhardt, R. J., and Mohammadi, M. (2000) Crystal structure of a ternary FGF−FGFR−heparin complex reveals a dual role for heparin in FGFR binding and dimerization, *Mol. Cell 6*, 743−750.
33. Fernandez-Tornero, C., Lozano, R. M., Redondo-Horcajo, M., Gomez, A. M., Lopez, J. C., Quesada, E., Uriel, C., Valverde, S., Cuevas, P., Romero, A., and Gimenez-Gallego, G. (2003) Leads for development of new naphthalenesulfonate derivatives with enhanced antiangiogenic activity: Crystal structure of acidic fibroblast growth factor in complex with 5-amino-2-naphthalene sulfonate, *J. Biol. Chem. 278*, 21774−21781.
34. Manetti, F., Cappello, V., Botta, M., Corelli, F., Mongelli, N., Biasoli, G., Borgia, A. L., and Ciomei, M. (1998) Synthesis and binding mode of heterocyclic analogues of suramin inhibiting the human basic fibroblast growth factor, *Bioorg. Med. Chem. 6*, 947−958.

BI051389B